Resistance to Degradation of Resin-Dentin Bonds Produced by One-Step Self-Etch Adhesives

Manuel Toledano,[1,*] Inmaculada Cabello,[1] Monica Yamauti,[1] Marcelo Giannini,[2] Fátima S. Aguilera,[1] Estrella Osorio,[1] and Raquel Osorio[1]

[1]University of Granada, Faculty of Dentistry, Dental Materials Section, Colegio Máximo de Cartuja s/n, 18071, Granada, Spain
[2]Piracicaba School of Dentistry, State University of Campinas, Piracicaba, Sao Paulo, Brazil

Abstract: The objective of this article is to evaluate the resistance to degradation of resin-dentin bonds formed with three one-step adhesives. Flat, mid-coronal dentin surfaces were bonded with the self-etching adhesives [Tokuyama Bond Force (TBF), One Up Bond F Plus (OUB), and G-Bond (GB)]. The bonded teeth were subjected to fatigue loading, chemical degradation, and stored in distilled water for four time periods (up to 12 months). Specimens were tested for microtensile bond strength and microleakage. Fractographic analysis was performed by scanning electron microscopy. Bonded interfaces were examined by light microscopy using Masson's trichrome staining. An atomic force microscope was employed to analyze phase separation and surface nanoroughness (Ra) at the polymers. Vickers microhardness and the degree of the conversion (DC) were also determined. ANOVA and multiple comparisons tests were performed. Bond strength significantly decreased after the chemical challenge, but not after load cycling. Aging decreased bond strength after 6 months in TBF and GB, in OUB after 12 months. An increase of the nonresin protected collagen zone occurred in all groups, after storing. TBF showed the highest roughness, microhardness, and DC values, and GB showed the lowest. Mild self-etch one-step adhesives (TBF/OUB) showed a higher degree of cure, lower hydrophilicity, and major resistance to degradation of resin-dentin bonds when compared to highly acidic self-etching adhesive (GB).

Key words: self-etch, adhesives, dentin, bonding efficacy, microleakage, surface properties

INTRODUCTION

Self-etching agents were introduced to eliminate the conditioning, rinsing, and drying steps, which are technique sensitive and difficult to standardize under clinical conditions (Tay et al., 1996). The self-etching systems can be presented as two-step with a separate etching-priming liquid, followed by the application of an adhesive resin or as simplified all-in-one adhesives that are used without a separate hydrophobic resin layer (Van Meerbeek et al., 2003). The latter have been introduced claiming easier and faster bond to tooth substrates in only one application (one-step), simplifying bonding procedures. However, these one-step adhesives are less effective than the etch-and-rinse or the two-step self-etch adhesives when applied to enamel (El Zohairy et al., 2010) or dentin (Van Landuyt et al., 2007). In these adhesives, hydrophobic and hydrophilic monomers are mixed together with a high content of solvent to keep them in solution (Van Landuyt et al., 2005). Most of these solvents are methacrylate-based and contain highly acidic monomers (pH around 1.5–2.5) (Moszner et al., 2005). Water-based highly acidic self-etching single-bottle adhesives arise from the hydrolytic instability of the methacrylate monomers used (i.e., HEMA) (Moszner et al., 2005). The occurrence of phase separation within the adhesive components and the formation of HEMA-containing hydrogels on the exposed collagen network have been recently

reported (Toledano et al., 2012*b*). Nevertheless, formulation of these adhesives can still be improved, with a bearing on bond durability.

To evaluate the bonding efficacy of dental adhesives, the microtensile test provides an assessment of the short-term bonding effectiveness of the adhesive by testing the response of the bonded interfaces to an acute stress (Pashley et al., 1999). However, teeth are continuously subjected to stresses during mastication, swallowing, and parafunctional habits. Weakly bonded tooth-material interfaces are more prone to suffer from the effects of oral environment in the short and long term (Erdilek et al., 2009). Among the different dental hard tissues, durable bonds to dentin are more difficult to achieve (Tay & Pashley, 2003). Proteolytic enzymes contained in the oral microflora and dentinal endogenous proteinases may also be potential sources of chemical degradation (Van Strijp et al., 2003). *In vitro* dynamic mechanical test and chemical challenge, possibly combined with aging methods, would add useful information for a more realistic prediction of the long-term stability and clinical behavior.

Therefore, the purpose of this study was to evaluate the resistance to degradation of resin-dentin bonds and enamel/dentin microleakage created by using three different one-step adhesive systems, and to determine the influence of the degree of conversion (DC), nanoroughness, and microhardness of these materials on the bonding efficacy. The null hypotheses tested are that there are no differences in dentin bond strength and bond resistance to degradation between the three tested one-step adhesive systems.

MATERIALS AND METHODS

Microtensile Bond Strength Test

Eighty-four unerupted human third molars, which were stored for less than 1 month in 0.5 chloramine T 1% at 4°C, were used for the study. Teeth were collected after the patients' informed consent under a protocol approved by the Institution Review Board. The specimens were sectioned below the dentin-enamel junction and ground flat (180-grit) under running water. Three one-step self-etch adhesives were employed (Table 1) according to the manufacturers' instructions, and a resin build-up, each 6 mm in height, was constructed from a hybrid composite (Tetric EvoCeram, shade A2, Ivoclar-Vivadent, Schaan, Liechtenstein). Each increment (1.5 mm) was light-activated for 40 s with a light-curing unit (Bluephase G2, Ivoclar-Vivadent). The light intensity output was monitored with a radiometer (Demetron Research Corporation, Danbury, CT, USA). Resin-bonded specimens were stored in deionized water at 37°C for 24 h, and they were divided into seven subgroups ($n = 4$). Subgroup a: no further treatment; teeth were vertically sectioned into beams with a cross-sectional area of 1 mm^2. Subgroup b: load cycling (5,000 cycles, 90 N). Subgroup c: load cycling (50,000 cycles, 90 N). These compressive loads were applied using a 5-mm-diameter spherical stainless steel plunger attached to a cyclic loading machine (model S-MMT-250NB, Shimadzu, Tokyo, Japan). After loading, the teeth were sectioned into beams. Subgroup d: teeth were sectioned into beams, which were immersed in 10% NaOCl$_{aq}$ solution (Panreac, Barcelona, Spain) for 5 h and rinsed in water for 1 h. Subgroup e: teeth were sectioned into beams and stored in distilled water for 3 months. Subgroup f: teeth were sectioned into beams and stored in distilled water for 6 months. Subgroup g: teeth were sectioned into beams and stored in distilled water for 12 months. To avoid enamel protection of resin-dentin bonds, dentin beams were immersed instead of the restored tooth (Toledano et al., 2007).

All dentin beams were then attached to a modified Bencor Multi-T testing apparatus (Danville Engineering, Danville, CA, USA) with a cyanoacrylate adhesive (Zapit, Dental Ventures of America, Corona, CA, USA). Beams were stressed to tensile failure in a universal testing machine (Instron 4411, Instron Corporation, Canton, MA, USA) at a crosshead speed of 0.5 mm/min. The bond strength values were calculated in MPa and analyzed using ANOVA and Student-Newman-Keuls multiple comparisons ($p < 0.05$). Fractured specimens were examined with a stereomicroscope (Olympus SZ-CTV, Olympus, Tokyo, Japan) at 40× magnification to determine the mode of failure. Failure modes were classified as cohesive in dentin or composite resin, adhesive, or mixed.

Scanning Electron Microscope Analysis

Representative specimens of each group were maintained for 48 h in a desiccator (Sample Dry Keeper Simulate Corp., Japan) and then mounted on aluminum stubs with carbon cement. They were then sputter-coated with pure gold by

Table 1. Composition and Mode of Application of the Tested Adhesives and Resin Composite.

Material (Code/Manufacturer/Batch Number)	pH	Composition	Mode of Application
Tokuyama Bond Force (TBF; Tokuyama Dental Corp., Tokyo, Japan, ET10157)	2.3	Methacryloyloxyalkyl acid phosphate, HEMA, bis-GMA, TEGDMA, water, isopropyl alcohol, glass fillers, CQ	Apply for 20 s, strong air blast. After gentle air blast, light cure for 10 s.
One Up Bond F Plus (OUB; Tokuyama Dental Corp., Tokyo, Japan, 017E89)	1.3	Adhesive A: MAC-10, MMA, HEMA, water, coumarin dye, methacryloyloxyalkyl acid phosphate. Adhesive B: multifunctional methacrylic monomer, fluoraluminosilicate glass, photoinitiator (arylborate catalyst)	Mix Bonding Agent A and Bonding Agent B until the mixed turns homogenously pink. Apply the mixture rubbing for 10 s. Light cure for 10 s.
G-Bond (GB; GC Corp., Tokyo, Japan, 0411221)	1.8	Phosphate ester monomer, 4-MET, UDMA, acetone, water, microfiller, photoinitiator	Apply for 10 s. Strong air blast for 3 s, light cure for 10 s.
Tetric Ceram (Ivoclar Vivadent, Schäan, Liechtenstein, L27365)		Paste of dimethacrylates, inorganic fillers, ytterbiumtrifluoride, initiators, stabilizers, and pigments <9% Bis-GMA <5% Triethylene glycoldimethacrylate <8% Urethanedimethacrylate	

means of a sputter-coating Unit E500 (Polaron Equipment Ltd., Watford, UK) and observed with a scanning electron microscope (SEM) at an accelerating voltage of 20 kV, to examine the microscopic fracture patterns and the morphology of the debonded interfaces.

Microleakage Test

Fifteen noncarious extracted human third molars were used. Two standardized Class V cavities were prepared on the buccal and lingual surfaces at the cementum-enamel junction, according to the procedure described by Toledano et al. (2000). The bonding agents were applied on enamel and dentin following manufacturer's recommendations (Table 1). Tetric Ceram resin composite was inserted in two oblique increments, light-cured, and restorations were carefully finished and polished with sof-lex discs (3M Dental Products, St. Paul, MN, USA). Specimens were stored in tap water at 37°C for 24 h. Groups were prepared for microleakage (ML) evaluation by coating the complete tooth with one application of nail varnish except for 1 mm around the restoration margin. The apices of the teeth were sealed with zinc-oxide eugenol cement. All specimens were then subjected to 500 temperature cycles (6°C/60°C; dwell time: 30 s). Subsequently, they were immersed in a 0.5% solution of basic fuchsine for 24 h at 37°C, rinsed with water, air dried, and invested in clear, epoxy resin. Each tooth was sectioned longitudinally in a buccolingual direction through the restorations with a low-speed water-cooled diamond saw.

ML of dye was observed in a stereomicroscope and recorded according to the following criteria: 0, no dye penetration; 1, dye penetration at the interface to one-half the depth of the cavity wall; 2, dye penetration to the full depth of the cavity wall, but not including the axial wall; 3, penetration to and along the axial wall. The worst value (maximum amount of leakage) recorded for each margin was selected for the analysis. The occlusal and gingival scores for each group of restorations were compared using the Kruskal-Wallis one way ANOVA and Mann-Whitney U nonparametric tests. Combined occlusal and gingival mean scores within each restoration were compared using the Wilcoxon matched pairs signed rank test ($p < 0.05$).

Atomic Force Microscopy Analysis and Nanoroughness Measurements

Four specimens of each adhesive system were performed. To shape the specimens (4.0 mm inner diameter $\times$ 1.0 mm thick), Teflon® molds covered with a clear glass plate were used. The samples were irradiated with a light-curing unit (Bluephase G2). The light guide was located in different position for the time of manufacturers' instructions, until the entire area was exposed. After removing the specimens from the molds, they were automatically polished wet on both sides (Struers LaboPol-4, Struers, Copenaghen, Denmark) using a series of SiC abrasive papers down to 4000 mesh. Subsequently, they were polished with diamond pastes of 1 and 0.25 μm on a hard

cloth and, finally, finished by polishing with 0.05-μm alumina powder slurry.

The disks surfaces were scanned using a tapping mode/atomic force microscopy (TM/AFM) (Nanoscope V, Digital Instruments, Veeco Metrology Group, Santa Barbara, CA, USA). The tapping mode was performed using a 1–10 Ohm-Cm phosphorus (n) doped Si tip. Changes in vertical position provide the height of the images, registered as bright and dark regions. The tip sample was maintained stable through constant oscillation amplitude. A data scale of 1,504 μm and a slow scan rate (0.1 Hz) were employed. Five phase images and five three-dimensional (3D) digital images (1.0 μm $\times$ 1.0 μm) in air were obtained from each specimen. To analyze the surface nanoroughness, five randomized boxes (300 nm $\times$ 300 nm) were created on each topographical image ($n = 75$). Topography and the average surface nanoroughness (Ra nanometers) of the scanned areas were evaluated. All measurements were performed using Nanoscope Software V7. Nanoroughness values (Ra nanometers) were analyzed by one-way ANOVA and Student-Newman-Keuls multiple comparisons tests.

Microhardness Measurements

Vickers microhardness was determined at the same adhesives surfaces after the AFM analysis. Measurements were done using an Instron Wolpert hardness tester (V-testor 4021, Instron Wolpert GmbH, Ludwigshafen, Germany) under loads of 300 g for 30 s for all the specimens. Fifteen indentations were analyzed by the reading of the long diagonal formed by the indenter. Distance between indentations was approximately twice the size of each indentation to minimize interactions between neighboring marks. Vickers hardness was calculated and expressed in Vickers hardness number (VHN) by examination of the surface with an optical microscope (200×) (Carl Zeiss, Oberkochen, Germany), according to the following formula:

$$\text{VNH} = \frac{1{,}854.4P}{d^2}, \qquad (1)$$

where P is the load in grams, and d is the mean diagonal of indentation in micrometers. Microhardness values were statistically analyzed with ANOVA and Student-Newman-Keuls was used for *post hoc* comparisons. Statistical significance was set at $p < 0.05$.

Light Microscopy—Masson's Trichrome Staining

After 24 h of water storage—5,000 cycles, 90N of load cycling; 50,000 cycles 90N of load cycling; 10% NaOCl$_{aq}$ solution immersion; 3 months of water storage, 6 months of water storage, and 12 months of water storage—the remaining nontrimmed slabs were used for the histomorphological evaluations. The medial aspects of each resin-dentin bonded slab was fixed in a glass holder with a photocuring adhesive (Technovit 7210 VLC, Heraeus Kulzer GmbH Co., Werheim, Germany) and ground with SiC papers of increasing fine grits (800, 1,000, 1,200, and 4,000) in a polisher (Exakt,

Table 2. Mean MTBS Results (MPa) and Percentage Distribution (%) of Failure Mode after Microtensile Bond Strength Testing for the Different Experimental Groups.

Experimental Groups	Failure Mode A	M	TBF	Failure Mode A	M	OUB	Failure Mode A	M	GB
24 h	14.3	85.7	32.12 (6.47) 1a	33.3	66.7	24.35 (7.10) 2a	81.5	18.5	14.14 (4.11) 3a
5,000 cycles	16.7	83.3	26.60 (6.82) 1a	69.2	30.7	22.18 (6.17) 1a	87	13	13.45 (4.28) 2a
50,000 cycles	31.6	68.4	28.82 (8.04) 1a	66.7	33.3	25.59 (8.43) 1a	90	10	12.16 (3.81) 2a
NaOCl	56	44	10.63 (3.15) 1b	16.1	83.9	10.13 (6.89) 1b	100	0	5.85 (2.23) 2b
3 months	3.27	67.3	31.02 (5.74) 1a	42.2	57.8	22.47 (7.42) 2a	84.8	15.2	13.00 (6.40) 3a
6 months	47.2	52.8	22.47 (5.84) 1b	38.7	61.3	22.10 (6.61) 1ab	91.2	8.8	7.79 (3.98) 2b
1 year	51.7	48.3	18.20 (5.99) 1b	43.4	56.6	13.90 (6.12) 1b	93.9	6.1	6.30 (3.70) 2b

Note: For each horizontal row: values with identical numbers indicate no significant difference using Student-Newman-Keuls test ($p > 0.05$). For each vertical column: values with identical letters indicate no significant difference using Student-Newman-Keuls test ($p > 0.05$).

Apparatebau D-2000, Norderstedt, Germany) until its thickness was approximately 10 μm. Slices were stained with Masson's trichrome for differentiation of resin and nonresin encapsulation of the exposed collagen. This dye has a high affinity for cationic elements of normally mineralized type I collagen, resulting in staining collagen green, and when demineralized, resulting in different coloration, generally red. With this staining technique, collagen coated with adhesive stains orange and pure adhesive appears beige. Slides with adherent stained sections were dehydrated through ascending ethanol and xylene. The sections were cover slipped and examined by light microscopy (BH-2, Olympus, Tokyo, Japan) at 100× magnifications. Three slices were prepared from each specimen, and images were digitalized in a scanner (Agfa Twin 1200, Agfa-Gevaert NV Mortsel, Belgium). In each specimen, the presence or absence of a red band (that would correspond to demineralized dentin) was observed. A qualitative assessment of the collagen encapsulation was completed by observing color differences within the interfacial zones of resin-dentin interfaces (Toledano et al., 2012a).

Degree of Conversion

For the DC analysis, the materials were manipulated according to the manufacturer's instructions at 25°C and placed on the center of a horizontal diamond element of an attenuated total reflectance attachment (Golden Gate, Specac, Woodstock, GA, USA) in the optical bench of a Fourier transform infrared spectrometry spectrometer (Tensor 27, Bruker Optik GmbH, Ettlingen, Germany). Thus, the diamond surface simulated the tooth surface to which the bonding agents were applied as the infrared beam penetrated the adhesives to a depth of approximately 2 μm. Adhesive tape was placed around the diamond element to act as a spacer, ensuring a standard thickness for all specimens (100–120 μm). The deposited material was covered with a Mylar strip and was either light activated following the manufacturers' instructions (Bluephase G2) through a glass slide (approximately 1 mm thick).

For analysis of the DC, the aliphatic carbon-to-carbon double bond absorbance peak intensity, located at 1,638 cm^{-1}, and that for the aromatic component, located

at 1,608 cm^{-1} (aromatic), were compared in each spectrum before and after the polymerization reaction, and monomer conversion was determined using the following equation (Ferracane & Greener, 1984):

$$DC = \frac{[abs\,(C=C\;alifatic)/abs\,(C \ldots aromatic)]\;polymer}{[abs\,(C=C\;alifatic)/abs(C \ldots aromatic)]\;monomer} \times 100,$$

where DC is the degree of conversion (%) and abs is the absorbance.

The DC was obtained by subtracting the percentage of the remaining carbon double bonds (% C=C) from 100%. To measure the effectiveness of the polymerization, the DC of each adhesive was determined at initial 2- and 5-min intervals. Only intrabrand conversion values were compared by one-way repeated measurements. One-way analysis of variance and the Student-Newman-Keuls *post hoc* test was employed to compare between adhesives. Statistical significance was established at $p < 0.05$.

RESULTS

Microtensile Bond Strength Test

The mean microtensile bond strength test (MTBS) values and failure modes obtained for the different groups are shown in Table 2. The adhesive type ($F = 12.32$; $P < 0.001$) and the challenging procedures ($F = 25.21$; $P < 0.001$) significantly affected the MTBS to dentin. Interactions between factors were also significant ($P < 0.05$). After 24 h of water storage, Tokuyama Bond Force (TBF) showed the highest bond strength values, and G-Bond (GB) the lowest. Load cycling did not produce significant changes in bond strength. MTBS decreased significantly when specimens were subjected to the NaOCl$_{aq}$ challenge, following the trend: TBF = OUB > GB. After 12 months of water storage, TBF and One Up Bond F Plus (OUB) attained similar bond strength, higher than that obtained by GB. Mixed fracture modes were frequently identified in all groups. No pure cohesive failures were observed in any group. Low bond strengths (i.e., GB) were associated with higher percentages of adhesive failures. In general, the number of adhesive
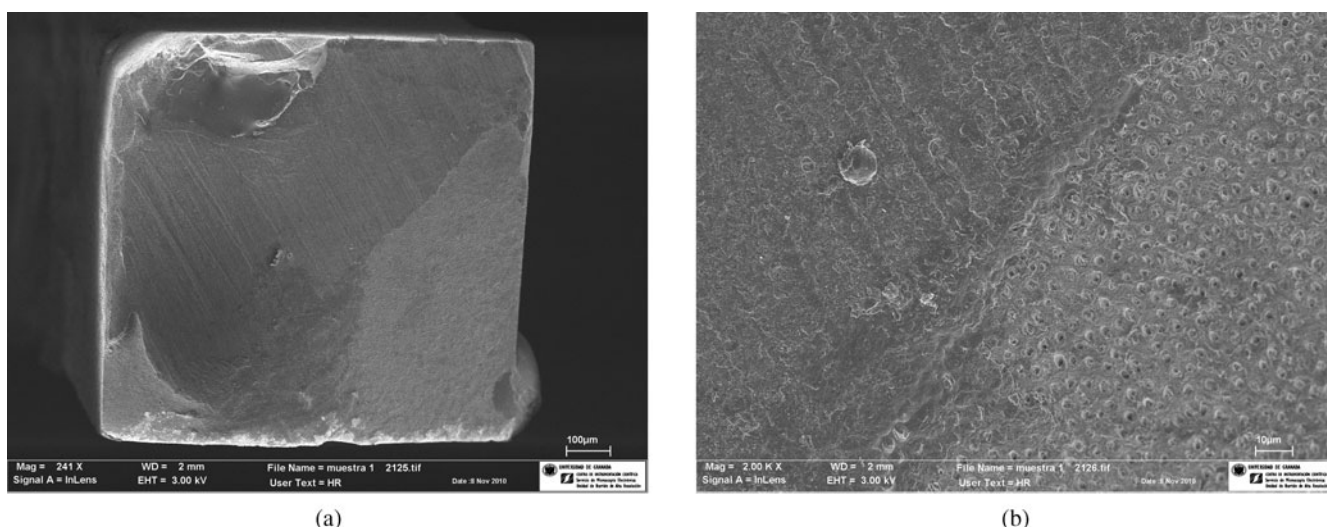
(a)

(b)

Figure 1. SEM observations of the fractured surface along the dentin side. Specimen bonded with TBF after 24 h of water storage, presenting a mixed failure (**a**). The failure was located both at the top and bottom of the hybrid complex. Scratches from the surface preparation were detected onto the hybrid complex. (**b**) At a higher magnification, peritubular dentin was observed and resin infiltration of intertubular dentin was evident.
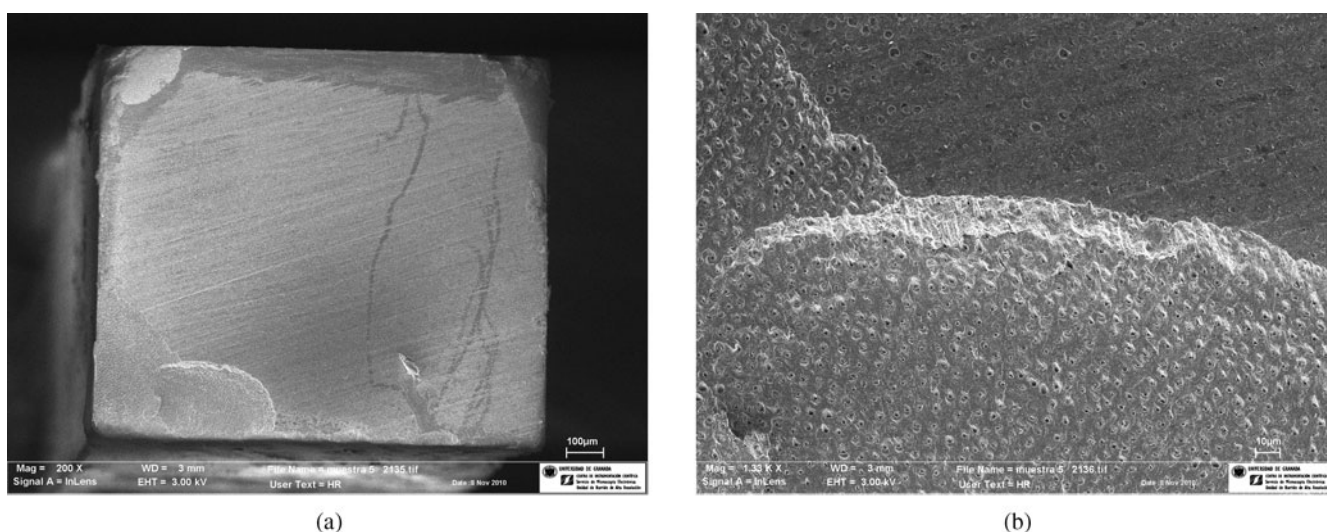

(a)

(b)

Figure 2. SEM observations of the fractured interface bonded with GB after 24 h of water storage, presenting a mixed failure (**a**). Numerous and little blisters along the fractured interface are evidenced. Some adhesive resin is remaining at the dentin surface. (**b**) Peritubular dentin and absence of resin tags are observed.

failures also increased with the challenge methods and with aging.

Scanning Electron Microscope Analysis

Debonded dentin surfaces are shown in Figures 1 to 5. Images from TBF (Fig. 1) and OUB specimens showed mixed failures at the top and at the base of the hybrid layer, after 24 h of storage. Specimens bonded with GB failed adhesively between both the dentin substrate and bonding layer (Fig. 2). The interfacial analysis of GB revealed a nonuniform thickness of the adhesive layer along the bonded interface. The presence of blisters was abundant, mainly entrapped at the bottom and in the middle of the resin layer. After mechanical loading, mixed failures were more frequent with TBF. OUB (Fig. 3) and GB showed predominantly adhesive failures, regardless the number of cycles. Mixed fracture modes showed partially cohesive failures within the adhesive resin in all groups. After $NaOCl_{aq}$ immersion, specimens showed partially cohesive failures within the adhesive resin (Figs. 4, 5). A gradual loss of adhesive from the periphery to the center portion of the bonding area was observed in all groups; the resin-remaining area was smaller for GB than for the rest of the adhesives. Intertubular dentin was clearly altered by $NaOCl_{aq}$ in all groups. After aging, partial cohesive fractures of demineralized dentin just below the hybrid layer were sometimes observed, mostly after 6 and 12 months of water storage. Resin was hardly observed on dentin surface after 12 months
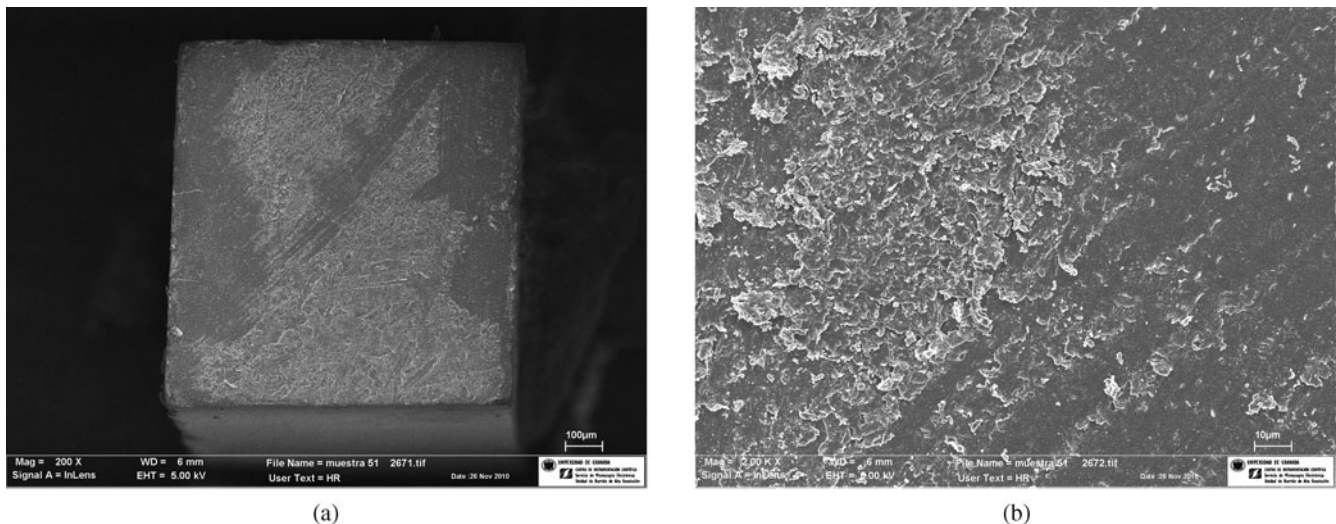
Figure 3. SEM image of an adhesive failure of a debonded dentin surface, after using OUB and 50,000 cycles of loading (**a**). The failure was found either within the hybridized smear layer or at the top of the hybrid complex, where scratches produced by the preparation of the bonding dentin surface with carbide papers were shown. (**b**) Intertubular dentin appeared covered and dentin tubules remained occluded by the fractured resin layer.
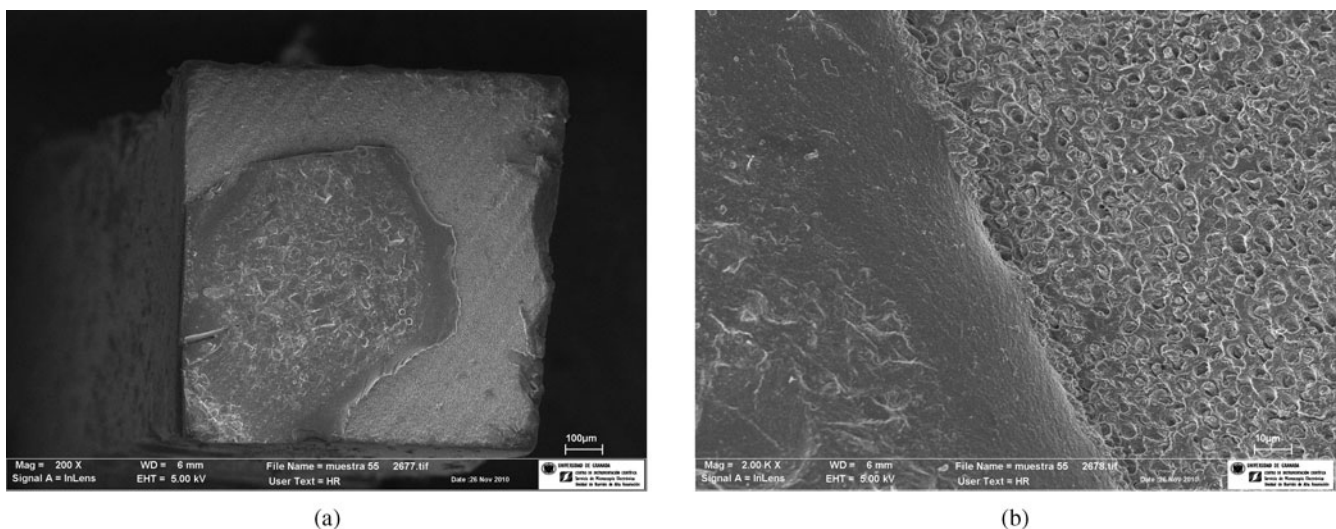

Figure 4. SEM image of the fractured dentin surface of a specimen bonded with TBF and debonded after $NaOCl_{aq}$ immersion (**a**). A mixed failure can be observed. The main fracture occurred at the top of the hybrid layer because of the loss of the adhesive resin. (**b**) Enlarged entrances of the dentinal tubules with scarce and poor resin tags are unveiled. Intertubular dentin seems porous and altered.

of water immersion, and the morphology of the intertubular dentin was altered as a result of the loss of the incompletely infiltrated collagen fibrils.

Microleakage Test

The results of the ML test are reported in Table 3. None of the teeth in any groups was completely free of ML. No significant differences among TBF and OUB adhesives were evident after 24 h, regardless of the evaluated margin. Regarding the enamel margin, GB attained the lowest ML. However, on gingival margins GB leaked significantly more than the other two tested adhesives.

Atomic Force Microscopy and Nanoroughness Measurements

AFM images are presented in Figures 6–8. Phase images revealed the different patterns of the polymer network and particles of the adhesive systems. Topographical 3D images exhibited the peaks and valleys produced by the nanoparticles aggregation. Mean nanoroughness values are displayed in Table 3. Mean nanoroughness was affected by the adhesive system ($F = 17.34$, $P < 0.001$). OUB exhibited significant lower roughness than TBF. GB nanoroughness could not be measured due to the scarce polymerization on the surface of the adhesive film.
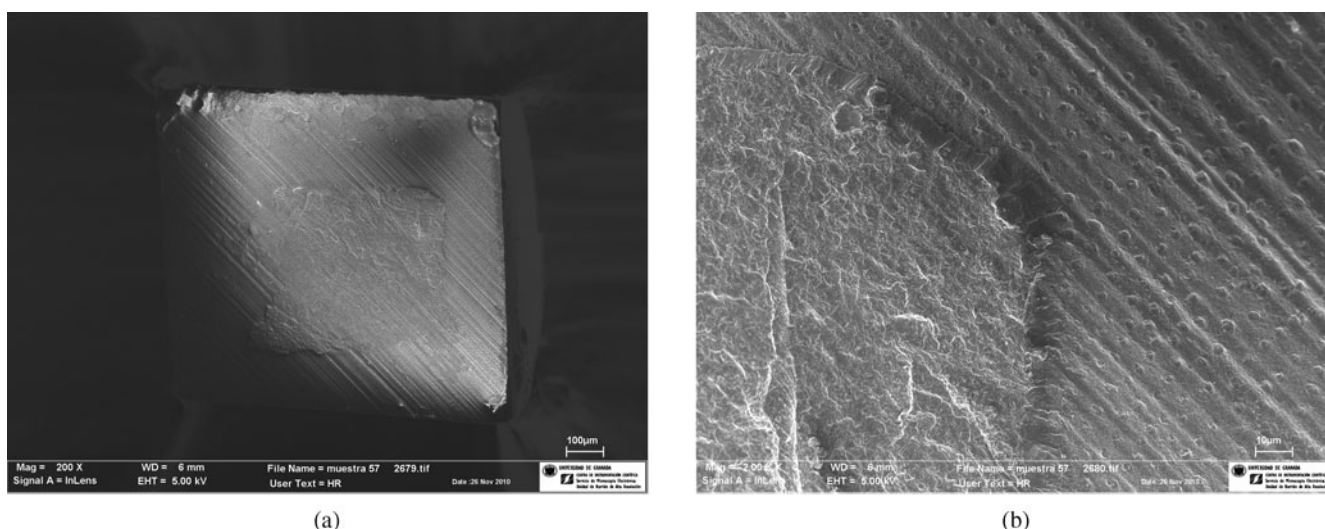
(a)

(b)

Figure 5. SEM image of the fractured dentin surface of a specimen bonded with OUB and debonded after $NaOCl_{aq}$ immersion. A mixed failure, at the bottom of the hybrid complex, may be observed (**a**). A large adhesive remaining area is observed at the central part of the specimen. Exposed dentin underlying the hybrid complex is shown (**b**). Some resin-filled dentinal tubules are observed.

Microhardness Measurements of Adhesives

The obtained mean values of Vickers microhardness are presented in Table 3. TBF revealed the highest surface hardness, significantly different from OUB. The lowest VHN values were observed in the GB adhesive system, with significant differences, when compared with the other two tested adhesives.

Light Microscopy—Masson's Trichrome Staining

Representative light micrographs of Masson's trichrome stained sections of the resin–dentin interfaces are presented in Figures 9–11. The extent to which the adhesive encapsulated the demineralized dentin matrix was reflected in the color differences within the stained sections. In these trichrome stains, mineralized dentin is stained green, exposed collagen is stained red, and pure adhesive is beige. TBF infiltrated dentin showed a degree of collagen encapsulation superior to that of OUB and GB. Nonuniform or discontinuous orange, pink, and red areas, below the adhesive interface, were also noticed, representative of demineralized and nonencapsulated dentin, especially when interfaces were challenged with $NaOCl_{aq}$ and 6 months of water immer-sions. These areas indicate that the structure of collagen has been altered. Six months of water storage produced a larger area of exposed collagen available to react with Masson's stain, ranging from an intense red fringe (Fig. 10c) to a pale red or pink area along the resin-dentin interface (Fig. 10a). A wide fringe of nonencapsulated and exposed collagen was also detectable in GB specimens, which showed the highest rate of debonded interfaces and bubbles formation through the adhesive layer. Load cycling, in general, did not change the chromatic appearance of Masson's stain.

Degree of Conversion

Percentages of DC and standard deviations are displayed in Table 4. Percentages of DC were affected by adhesive system ($F = 14.78$; $P < 0.001$) and by the time intervals ($F = 11.32$; $P < 0.001$). Interactions were also significant ($P < 0.05$). There are differences between the adhesive systems in all the time intervals. TBF exhibited the highest percentage DC and GB showed the lowest. No differences were shown between the interval times 2 and 5 min in TBF adhesive system, with the initial percentage of DC being the lowest

Table 3. (**a**) Microleakage Scores Obtained for Each Adhesive System. (**b**) Means and Standard Deviations (SD) of Roughness Values (Ra-nm) of the Adhesive Surfaces. (**c**) Mean and Standard Deviations (SD) Microhardness Measurements—VHN—Attained for Each Adhesive System.

Adhesive Systems	(a) Microleakage										(b)	(c)
	Enamel					Dentin						
	0	1	2	3	n	0	1	2	3	n	Nanoroughness	Microhardness
TBF	2	8	0	0	10A	1	3	3	3	10A	4.21 (1.33) a	27.60 (2.68) A
OUB	2	7	1	0	10A	1	3	2	4	10A	0.65 (0.44) b	22.36 (2.98) B
GB	7	2	1	0	10B	0	1	3	6	10B	—	8.76 (1.81) C

Note: Values with the same letters are not significantly different ($p > 0.05$). For microleakage table: Same letters indicate not significant differences in columns between adhesive groups ($P < 0.05$). In all groups, enamel obtained significantly less microleakage than dentin.
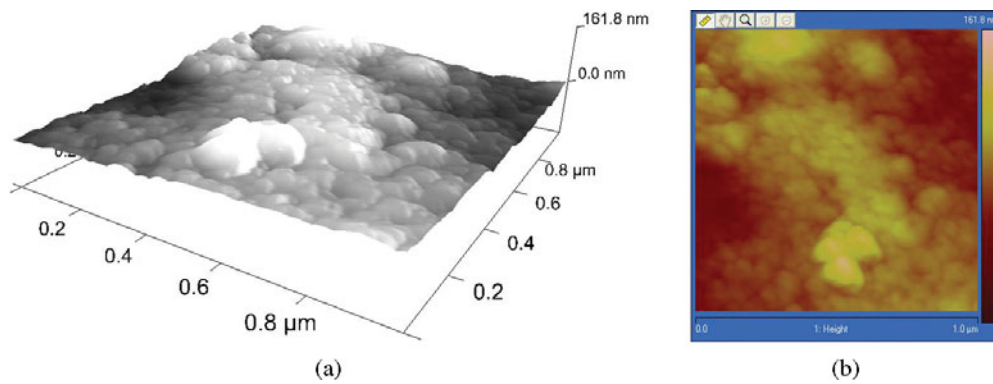
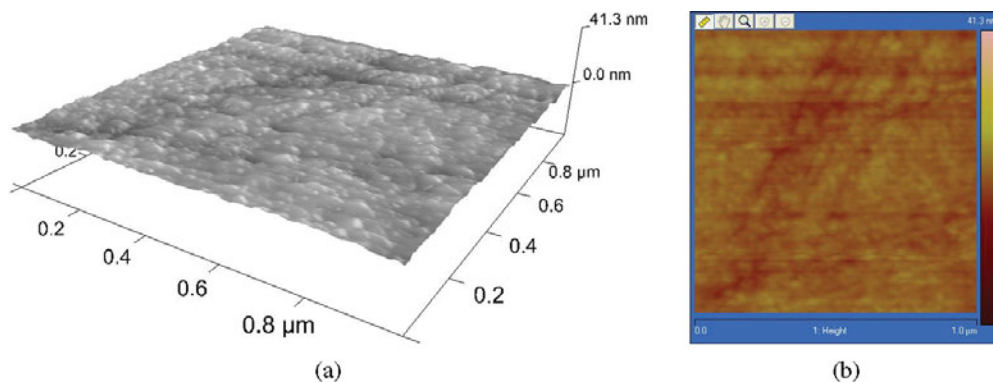**Figure 6.** 3D and phase images of the adhesive system TBF.

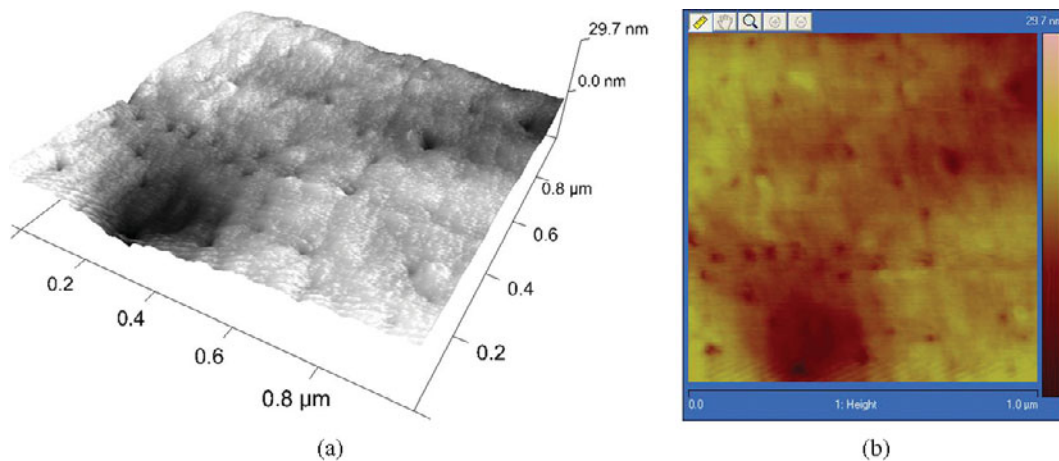**Figure 7.** 3D and phase images of the adhesive system OUB.

Figure 8. 3D and phase images of the adhesive system GB.

value. All adhesives presented augmented percentage of DC when time interval increased.

A combined graph with MTBS mean values in different experimental groups and DC values is presented in Figure 12.

DISCUSSION

The most common methods that are used to evaluate adhesion to restorative materials to dentin and enamel involve measuring the bond strength to tooth-restorative interfaces and by testing the marginal seal of restorations in extracted

teeth. The ideal adhesive restorative material would produce high bond strength and no ML (Gordan et al., 1997). In the present study, different experiments were combined to ascertain the factors affecting resistance to degradation of one-step adhesives. It is the first study showing such ample amount of different testing experiments of bonding efficacy.

TBF attained the highest and GB the lowest bond strength values after 24 h of water storage (Table 2). TBF and GB also showed more frequently mixed and adhesive failures, respectively (Table 2; Figs. 1, 2). On the other hand, TBF and OUB attained similar leakage scores in both enamel
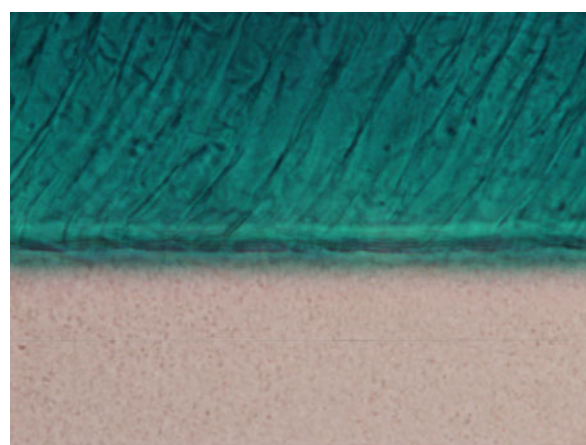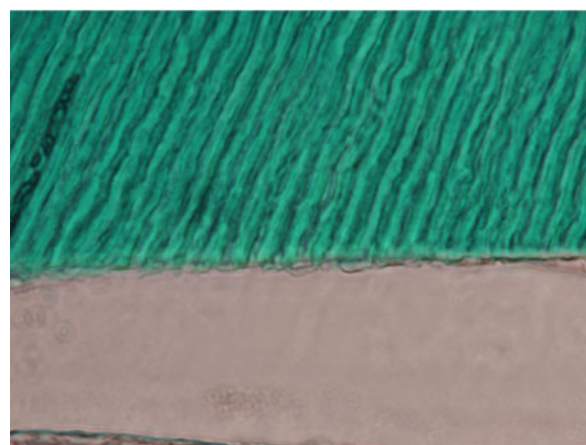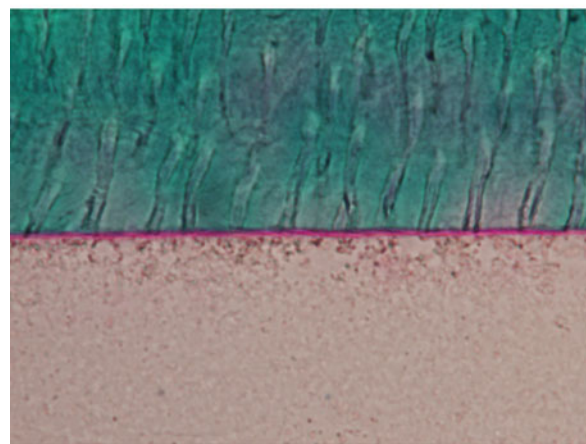
Figure 9. Representative light micrographs of TBF specimen's interface stained with Masson's trichrome: mineralized dentin stained green, adhesive stained beige, and exposed protein stained red. Original magnification: 100×. (**a**) TBC after 24 h of water immersion; (**b**) TBF after NaOCl immersion; (**c**) TBF after 6 months of water immersion. Clear adhesive encapsulation (**a**) was noticed after 24 h. Slight and limited resin uncovered decalcified dentin was detected after NaOCl and 6 months of water immersions (**b**, **c**), as indicated by the enhancement of pink-orange and clear red zones along the length of the bonded interfaces and intertubular dentin.

Figure 10. Representative light micrographs of OUB specimen's interface stained with Masson's trichrome: mineralized dentin stained green, adhesive stained beige, and exposed protein stained red. Original magnification: 100×. (**a**) OUB after 24 h of water immersion; (**b**) OUB after NaOCl immersion; (**c**) OUB after 6 months of water immersion. Some mild-orange and red areas were observed at the resin-dentin interface unveiling a nonresin protected decalcified dentin, after 24 h of water and NaOCl immersions. After 6 months of water immersion, a thicker demineralized substrate (red and pink fringe) appeared, being wider than in the other two groups (24 h and NaOCl immersions).
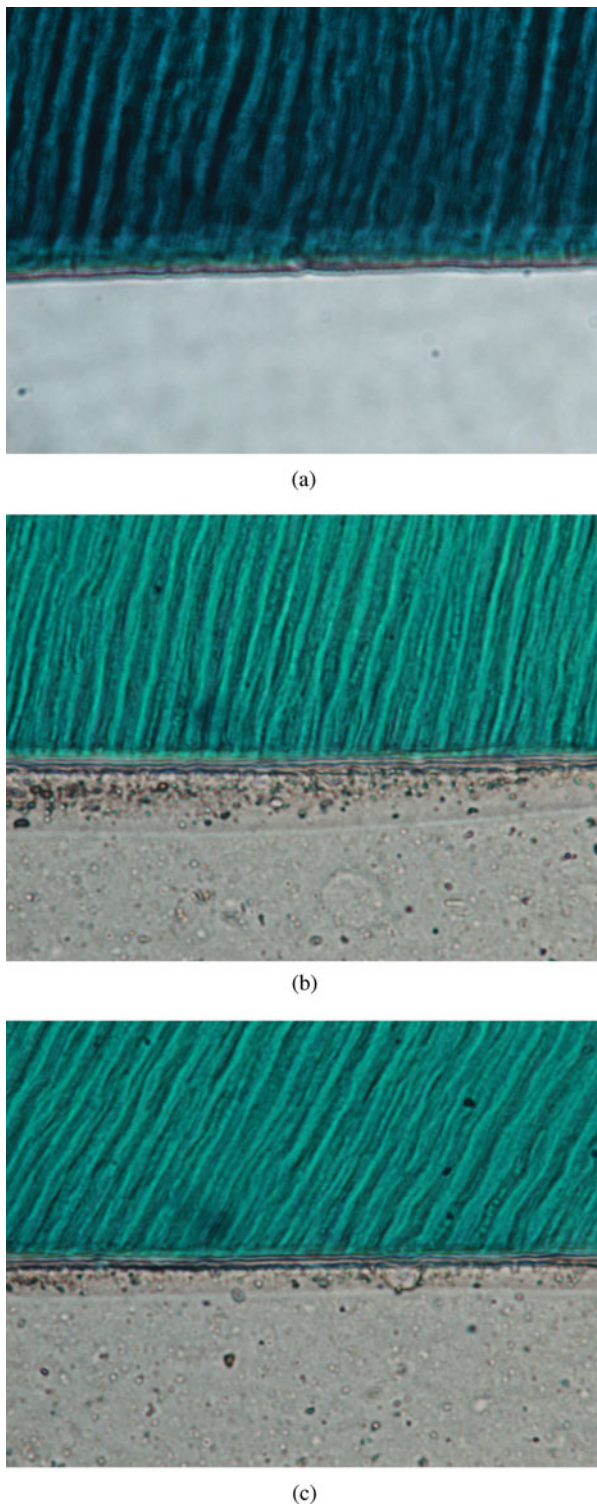
and dentin, but lower than GB, which showed the lowest sealing ability (Table 3a). When using U-shaped cavities, similar contraction stress is assumed to be generated both at the enamel and dentin margins; therefore, leakage may have occurred at both margins, especially because of the controversial enamel bond strengths of these self-etching systems (Osorio et al., 2005).

Differences in bond strength do not necessarily correlate with ML results. Bonding efficacy is influenced by both the type of acidic monomer and the solvent content (Moszner et al., 2005). Acidic monomers are esters originating from the reaction of a bivalent alcohol with methacrylic acid and phosphoric/carboxylic acid derivatives. Each self-etch adhesive contains its specific functional monomer that, to a large extent, determines its actual adhesive performance (Yoshida et al., 2004a, 2004b). With regard to acidity of adhesive solutions, TBF with a pH of 2.3 (Table 1) can be categorized as a mild self-etch, whereas OUB and GB would be regarded as more aggressive solutions. Nevertheless, this different acidity does not appear as a determinant factor for bond strength (Margvelashvili et al., 2010). TBF contains a 3D self-reinforcing monomer, with several functional groups per molecule, enabling a multiple point interaction with dentin calcium (Takahashi et al., 2010) that also confers to the system the highest values of nanoroughness (Table 3b). This high nanoroughness value reflects the influence of cluster formation (Osorio et al., 2012) on surface properties. The bond strength and the surface roughness of adhesives were found to be related, assuming two factors that influence this relationship: (1) the effect of surface area and (2) the notch effect due to the surface roughness (Uehara & Sakurai, 2002). TBF showed the highest values of both nanoroughness and bonding efficacy (Tables 2, 3). Figure 6 may unveil the influence of the area effect and notch effect on the bonding strength and ML values, mainly assigned to the increase on the contact surface (Santos et al., 2007). TBF also showed the highest microhardness (Table 3c) and DC values, when compared with the other two adhesives (Table 4). The mechanical properties of cured adhesive resins may indirectly reflect the quality of curing (Takahashi et al., 2002) and may have a profound influence on the resin-dentin bond strength (Hass et al., 2011) (Fig. 12). The better performance of TBF may also result from the high degree of collagen encapsulation reflected in light microscopy examination (Fig. 9a). GB includes 4-MET that establishes a less intense ionic bond with

Figure 11. Representative light micrographs of GB specimen's interface stained with Masson's trichrome: mineralized dentin stained green, adhesive stained beige, and exposed protein stained red. Original magnification: 100×. (**a**) GB after 24 h of water immersion; (**b**) GB after NaOCl immersion; (**c**) GB after 6 months of water immersion. GB presented the highest rate of debonded interfaces. Red and purple lines and spots were observed along the base of the hybrid complex. Entrapped blisters and bubbles may be identified within the adhesive layer, especially after NaOCl and 6 months of storage.

Table 4. Percentage (%) of Degree of Conversion (DC) and Standard Deviation (SD) of Each Adhesive System.

Adhesive	DC Initial	DC 2 min	DC 5 min
TBF	68.3 (1.8) A1	77.0 (1.1) B1	79.1 (1.7) B1
OUB	42.5 (0.8) A2	57.1 (3.1) B2	60.4 (1.6) C2
GB	24.4 (0.8) A3	35.5 (0.7) B3	37.2 (0.8) C3

Note: Within the same column, percentages with identical number indicates no differences ($p > 0.05$); for each row, matching letters indicate no differences ($p > 0.05$).
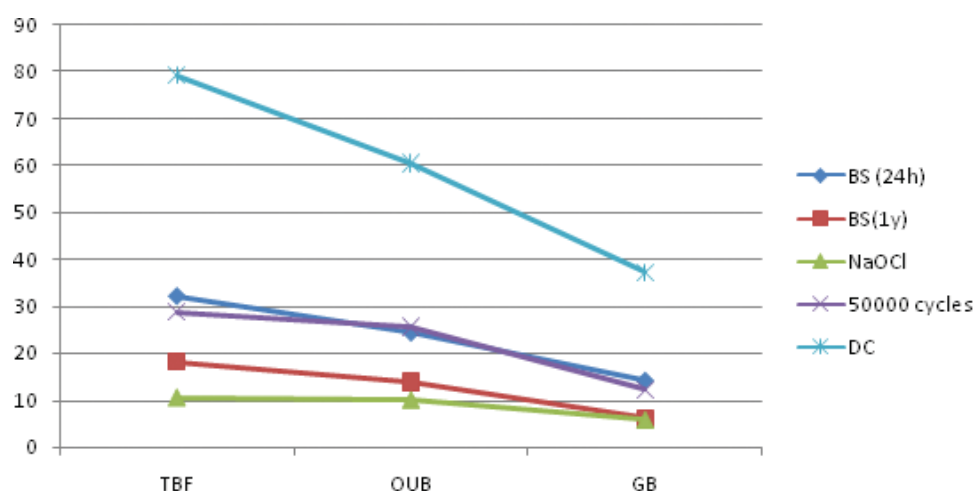
Figure 12. Mean MTBS results (MPa) for the different experimental groups and percentage of DC for the different tested adhesives.

calcium in hydroxyapatite, resulting a Ca-4MET salt with a relatively high solubility and low stability (Van Landuyt et al., 2007); therefore, chemical bonding potential on its own is not sufficient to assure adequate bonding performance (Yoshida et al., 2004b) as the calcium salt of 4-MET is easily dissolved.

All-in-one self-etch adhesives are complex mixtures containing water/solvents, hydrophilic and hydrophobic monomers as ingredients to promote effective acid-etching and resin-dentin bonding (Tay & Pashley, 2003; Van Landuyt et al., 2005). Consequently, they are intrinsically hydrophilic owing to the presence of acidic and highly polar functional groups substituted on methacrylates (Hosaka et al., 2010). The presence of water is essential for providing an ionization medium for self-etching activity (Tay & Pashley, 2001; Schulze et al., 2005). Water is not miscible with many constituents of self-etching adhesive and hence is combined with alcohol in TBF and OUB (Hosaka et al., 2010) or with acetone in GB. Water-alcohol mixtures promoted the formation of hydrogen bonds between water and ethanol molecules, leading to a better evaporation of these water-ethanol aggregates than pure water (Van Landuyt et al., 2007). Ethanol can maintain wide interfibrillar spaces after evaporation of the solvent, helping resin encapsulation (Fig. 9a). It has been demonstrated that higher bond strengths correlated with wider interfibrillar spaces, and such spaces should be properly infiltrated with resin (Eddleston et al., 2003). Therefore, acetone evaporates faster than ethanol/water, making difficult the total removal of water, leaving wet the interfibrillar spaces (Monticelli et al., 2007), further affecting the infiltration of resin monomers, compromising the resin encapsulation of the demineralized dentin. GB promoted, as a consequence, a nonuniform and discontinuous interface that exhibited pink and red areas below the adhesive layer with multiple entrapped blisters and bubbles (Figs. 2, 11a). Additionally, the application of acetone produces little solvation force, while alcohol produces higher solvation pressures that develop at increasing rates (Pashley et al., 2002).

OUB attained intermediate bond strength values, but closer to TBF. This adhesive system contains MAC-10 and HEMA as main monomer and solvent, respectively. MAC-10 includes a spacer group consisting of 10 carbon atoms, making this monomer rather hydrophobic, and conferring hydrolytic stability to the adhesive system (Van Landuyt et al., 2007) up to 12 months (Table 2). Additionally, OUB's initiator system contains dye-sensitizer, co-initiator, and the borate derivative. The energy transfer reaction from the dye-sensitizer to the co-initiator takes place by light irradiation to form an excited state of the co-initiator. Following this, the polymerizable radical species is formed by reaction of the borate derivative with the activated co-initiator containing hydrogen ions coming from the dye-sensitizer and acidic functional monomers (Miyazaki et al., 2002). This blend confers to the system some pattern of polymerization ability (Uekusa et al., 2006) and mechanical stability, as confirmed by the results that the present study provided (Tables 3c, 4). HEMA is a solvent that generally improves miscibility of hydrophobic and hydrophilic components in adhesive blends (Moszner et al., 2005; Van Landuyt et al., 2005), preventing phase separation (Van Landuyt et al., 2005). However, HEMA increases the hydrophilicity of adhesives, resulting in increase of water sorption and solubility of adhesive copolymers (Ito et al., 2005), producing microcracks through repeated sorption/desorption cycles, and originating a nonresin protected decalcified dentin. The resin-dentin interface appeared as mild-orange and red as result of poor resin encapsulation (Fig. 10a). After debonding, most specimens exhibited mixed failures (Table 2), frequently failing at the top of the hybrid layer with evidence of a more aggressive etching.

The omission of HEMA from the adhesive blends has been considered advantageous in removing water, separating it from the other components upon solvent evaporation (Van Meerbeek et al., 2005). However, if HEMA is absent from the adhesive blend, a higher solvent content is necessary to maintain components in solution. In this

study, TBF and OUB are HEMA-containing adhesives, while GB is a HEMA-free adhesive. GB contains high a amount of acetone (35–45%) as a solvent, theoretically, resulting in a better evaporation of water due to the "azeotropic effect" (Moszner et al., 2005) or "water-chasing effect" (Jacobsen & Söderholm, 1995) of acetone. The acetone content of GB adhesive system may have promoted water to move from the smear layer-covered dentin, leading to droplet formation (Hiraishi et al., 2007) (Fig. 2a). Transudation of fluids from the opened tubules (Fig. 2b) may be not the unique source of water within the hybrid layers, as phosphate and aqueous calcium have been recently recognized as by-products of hydroxylapatite dissolution when self-etching systems are applied (Monticelli et al., 2007). Although acetone is considered extremely volatile (Glavchev et al., 2003) and a good solvent for methacrylates (Zhou et al., 2001), its rapid evaporation from the adhesive blend brings a decrease in solvent-resin affinity and the formation of a monomer-rich phase, which may promote cross-linking (Yiu et al., 2005) and phase separation of water and monomers. With acetone evaporation exceeding that of water (Zhou et al., 2001; Hiraishi et al., 2007), the aqueous fraction accumulated in the adhesive film tends to increase (Fig. 2a), decreasing the degree of conversion (Table 4), negatively affecting the MTBS, contributing to de-bonding between dentin and bond layer, and increasing the percentage of adhesive failures (Table 2). This lower degree of cure of GB (Table 4) may also be due to a major solvent/oxygen inhibition effect in the photopolymerization (Nunes et al., 2005), leading to a lack of nanoroughness measurements (Table 3b) (Fig. 8) and to rapid degradation of the resin-dentin bonds (Hashimoto et al., 2002), decreasing its bonding efficacy after 6 months of water storage (Table 2).

Accelerated *in vitro* aging tests for resin-dentin bonds (both mechanical and chemical) may be crucial to evaluate the long-term stability of these interfaces under more clinically relevant conditions. *In vitro* cyclic loading simulates mechanical stresses at the bonded interfaces (Li et al., 2002) and did not influence on bond strength values after 5,000 nor 50,000 loading cycles. Because of this, the null hypothesis must be, partially, accepted. This could be attributed to incompletely polymerized resin in the hybrid layer (De Munck et al., 2003), as well as to internal voids within the adhesive layer that may have acted as a "stress releaser," reducing stress transmission to the underlying dentin (Monticelli et al., 2007). Moreover, it has been suggested that the presence of hydrophilic comonomers and their tendency to absorb water after polymerization may plasticize the resin-dentin interface enough to tolerate cyclic mechanical stressing without fracturing. Additionally, it has been stressed that all-in-one adhesives promote a deeper demineralization layer (Carvalho et al., 2005), which may distribute stresses over a greater volume of collagen, thereby lowering stress concentration (Sauro et al., 2011).

After loading, TBF and OUB performed similarly, showing higher bond strength than GB. The existence of a gradient of elasticity between the interdiffusion zone and the subjacent dentin when using these adhesive systems (TBF and OUB) may be important to withstand the load forces (Hosoya, 2006). This adhesive elastic area has the capacity to relieve major stresses between the composite restoration and the dentin substrate. The incomplete infiltration of the resin into GB-treated dentin, which exposes collagen at the base of the hybrid layer and the detection of many droplets at the resin-dentin interface (Monticelli et al., 2007), may have resulted in a hybrid layer that was much less stiff than the overlying adhesive layer. This mismatch in moduli of elasticity between the two layers may have caused the de-bonding between the insufficiently infiltrated dentin and the adhesive layer. Nevertheless, load cycling did affect the failure mode. It is observed at the SEM micrographs that the loading stress seemed to have been concentrated mostly at the interface between the adhesive and the hybrid layer and within the hybrid layer when using TBF, whereas specimens bonded using GB and OUB (Figs. 3a, 3b) mostly failed at the top of, or beneath, the hybrid layer. In both, the adhesive failed to envelop the collagen network, as observed by the presence of red and pink areas between the mineral dentin and the hybrid layer (Figs. 10a, 11a).

The durability of bonds between adhesive resin and dentin is crucial, and little is known regarding the stability of hybridized smear layers because their only retention to the underlying hybrid layer is via delicate ribbons of resin (Sano et al., 1999). Our results (Table 2) confirm a global decrease in bonding efficacy, especially from 6 months of water immersion. In general, dentin bond strength decreased during water storage over time because the degradation of collagen fibrils within the hybrid layer (De Munck et al., 2003) throughout a proteolytic degradation process. Immersion of the specimens in 10% sodium hypochlorite aqueous solution for a short experimental time period permits evaluation of the ability of the resin monomers to protect the collagen matrix of dentin from proteolytic activity (Yoshida et al., 2004b). After storage in NaOCl$_{aq}$, MTBS values were lower than those obtained after 24 h (Fig. 12). NaOCl$_{aq}$ is a nonspecific deproteinizing agent with the tendency of forming superoxide radicals in aqueous solutions, thus inducing oxidation phenomena that fragment the proteins peptide chains (Osorio et al., 2005; Monticelli et al., 2007). The NaOCl$_{aq}$ solution may affect the resin-dentin bond structures following two different pathways: (1) the etched and nonresin infiltrated layer and (2) the collagen that was not properly resin-infiltrated and/or later exposed because of the resin dissolution by the NaOCl$_{aq}$ solution (Toledano et al., 2006). Therefore, collagen fibrils in the conditioned dentin and the resin agent might have been affected by NaOCl$_{aq}$ action, leading to a rapid degradation of the adhesive-dentin layer (Yoshida et al., 2004a), thus explaining the lower MTBS values. Analysis of debonded sticks of specimens showed a gradual loss of adhesive at the top of the hybrid layer and within the adhesive resin (Figs. 4a, 4b); this loss of adhesive was from the periphery to the center of the debonded area. The SEM

analysis of the fractured surfaces bonded with these adhesives also revealed an aggressive action of NaOCl solution on the microstructure of the intertubular dentin (Figs. 4, 5). The resin tags were found to protrude, and the altered dentin surface suggested resin and collagen dissolution. It is clear from the results of this study that the presence of different functional monomers may influence the performance of the adhesive systems when submitted to chemical challenge. Thus, the test null hypothesis that NaOCl$_{aq}$ immersion does not affect bond strength to dentin must be rejected.

Obtained reduction in MTBS was similar to the decline in bond strength obtained when *in vivo* degradation studies were performed (Hashimoto et al., 2000). Bonding deterioration was also reflected in a relative higher percentage of adhesive failures obtained after MTBS testing. This drop in bonding efficacy may be the consequence of high solubility of adhesives and/or the existence of unprotected collagen fibrils within the hybrid layer (Osorio et al., 2005). Additionally, the lower monomer conversion of the adhesive resin and the existence of the residual water and voids have been pointed out as sources for this drop in bonding efficacy (Yamauti et al., 2003). *In vitro* simulations of clinical conditions under which dental substrates would fail are difficult because the factors involved in bond degradation *in vivo* are numerous, and not completely known.

One of the main factors affecting resistance to degradation of one-step self-etch adhesives is related to their excessive hydrophilicity that makes the adhesive layer more prone to attract water from dentin. Small droplets can be found at the hybrid layer, permeability of these adhesives contributes to the hydrolysis of resin polymers, and lower resistance to degradation of the hybrid layer is encountered. In general, it seems that the mild one-step self-etch adhesives performed better and possess a higher degree of cure, less hydrophilicity, and higher resistance to degradation (Fig. 12). However, clinical studies, even though they are time-consuming, expensive, and lack control over important variables, are necessary to confirm the improved resistance to degradation of these adhesives.

Acknowledgments

References

Carvalho, R.M., Chersoni, S., Frankenberger, R., Pashley, D.H., Prati, C. & Tay, F.R. (2005). A challenge to the conventional wisdom that simultaneous etching and resin infiltration always occurs in self-etch adhesives. *Biomaterials* **26**, 1035–1042.

De Munck, J., Van Meerbeek, B., Satoshi, I., Vargas, M., Yoshida, Y., Armstrong, S., Lambrechts, P. & Vanherle, G. (2003). Microtensile bond strengths of one- and two-step self-etch adhesives to bur cut enamel and dentin. *Am J Dent* **16**, 414–420.

Eddleston, C.L., Hindle, A.R., Agee, K.A., Carvalho, R.M., Tay, F.R., Rueggeberg, F.A. & Pashley, D.H. (2003). Dimensional changes in acid-demineralized dentin matrices following the use of HEMA-water versus HEMA-alcohol primers. *J Biomed Mater Res A* **67**, 900–907.

El Zohairy, A.A., Saber, M.H., Abdalla, A.I. & Feilzer, A.J. (2010). Efficacy of microtensile versus microshear bond testing for evaluation of bond strength of dental adhesive systems to enamel. *Dent Mater* **26**, 848–854.

Erdilek, D., Dörter, C., Koray, F., Kunzelmann, K.H., Efes, B.G. & Gomec, Y. (2009). Effect of thermo-mechanical load cycling on microleakage in class II ormocer restorations. *Eur J Dent* **3**, 200–205.

Ferracane, J.L. & Greener, E.H. (1984). Fourier transform infrared analysis of degree of polymerization in unfilled resins—Methods comparison. *J Dent Res* **63**, 1093–1095.

Glavchev, I., Nikolov, R.N. & Valchev, P. (2003). Determination of evaporation rates of mixed solvents with the formation of thin films for membranes. *Polym Test* **22**, 529–532.

Gordan, V.V., Vargas, M.A., Cobb, D.S. & Denehy, G.E. (1997). Evaluation of adhesive systems using acidic primers. *Am J Dent* **10**, 219–223.

Hashimoto, M., Ohno, H., Kaga, M., Endo, K., Sano, H. & Oguchi, H. (2000). *In vivo* degradation of resin-dentin bonds in humans over 1 to 3 years. *J Dent Res* **79**, 1385–1391.

Hashimoto, M., Ohno, H., Kaga, M., Sano, H., Endo, K. & Oguchi, H. (2002). The extent to which resin can infiltrate dentin by acetone-based adhesives. *J Dent Res* **81**, 74–78.

Hass, V., Folkuenig, M.S., Reis, A. & Loguercio, A.D. (2011). Influence of adhesive properties on resin-dentin bond strength of one-step self-etching adhesives. *J Adhes Dent* **13**, 417–424.

Hiraishi, N., Breschi, L., Prati, C., Ferrari, M., Tagami, J. & King, N.M. (2007). Technique sensitivity associated with air-drying of HEMA-free, single-bottle, one-step self-etch adhesives. *Dent Mater* **23**, 498–505.

Hosaka, K., Nakajima, M., Takahashi, M., Itoh, S., Ikeda, M., Tagami, J. & Pashley, D.H. (2010). Relationship between mechanical properties of one-step self-etch adhesives and water sorption. *Dent Mater* **26**, 360–367.

Hosoya, Y. (2006). Hardness and elasticity of bonded carious and sound primary tooth dentin. *J Dent* **34**, 164–171.

Ito, S., Hashimoto, M., Wadgaonkar, B., Svizero, N., Carvalho, R.M., Yiu, C., Rueggeberg, F.A., Foulger, S., Saito, T., Nishitani, Y., Yoshiyama, M., Tay, F.R. & Pashley, D.H. (2005). Effects of resin hydrophilicity on water sorption and changes in modulus of elasticity. *Biomaterials* **26**, 6449–6459.

Jacobsen, T. & Söderholm, K.J. (1995). Some effects of water on dentin bonding. *Dent Mater* **11**, 132–136.

Li, H., Burrow, M.F. & Tyas, M.J. (2002). The effect of load cycling on the nanoleakage of dentin bonding systems. *Dent Mater* **18**, 111–119.

Margvelashvili, M., Goracci, C., Beloica, M., Papacchini, F. & Ferrari, M. (2010). *In vitro* evaluation of bonding effectiveness to dentin of all-in-one adhesives. *J Dent* **38**, 106–112.

Miyazaki, M., Tsubota, K., Onose, H. & Hinoura, K. (2002). Influence of adhesive application duration on dentin bond strength of single-application bonding systems. *Oper Dent* **27**, 278–283.

Monticelli, F., Osorio, R., Pisani-Proença, J. & Toledano, M. (2007). Resistance to degradation of resin-dentin bonds using a one-step HEMA-free adhesive. *J Dent* **35**, 181–186.

Moszner, N., Salz, U. & Zimmermann, J. (2005). Chemical aspects of self-etching enamel-dentin adhesives: A systematic review. *Dent Mater* **21**, 895–910.

Nunes, T.G., Ceballos, L., Osorio, R. & Toledano, M. (2005). Spatially resolved photopolymerization kinetics and oxygen inhibition in dental adhesives. *Biomaterials* **26**, 1809–1817.

Osorio, E., Toledano, M., Yamauti, M. & Osorio, R. (2012). Differential nanofiller cluster formations in dental adhesive systems. *Microsc Res Tech* **75**, 749–757.

Osorio, R., Toledano, M., Osorio, E., Aguilera, F.S. & Tay, F.R. (2005). Effect of load cycling and *in vitro* degradation on resin-dentin bonds using a self-etching primer. *J Biomed Mater Res A* **72**, 399–408.

Pashley, D.H., Carvalho, R.M., Sano, H., Nakajima, M., Yoshiyama, M., Shono, Y., Fernandes, C.A. & Tay, F. (1999). The microtensile bond test: A review. *J Adhes Dent* **1**, 299–309.

Pashley, D.H., Carvalho, R.M., Tay, F.R., Agee, K.A. & Lee, K.W. (2002). Solvation of dried dentin matrix by water and other polar solvents. *Am J Dent* **15**, 97–102.

Sano, H., Yoshikawa, T., Pereira, P.N., Kanemura, N., Morigami, M., Tagami, J. & Pashley, D.H. (1999). Long-term durability of dentin bonds made with a self-etching primer, *in vivo*. *J Dent Res* **78**, 906–911.

Santos, P., Júlio, E. & Silva, V. (2007). Correlation between concrete-to-concrete bond strength and the roughness of the substrate surface. *Constr Build Mater* **21**, 1688–1695.

Sauro, S., Toledano, M., Aguilera, F.S., Mannocci, F., Pashley, D.H., Tay, F.R., Watson, T.F. & Osorio, R. (2011). Resin-dentin bonds to EDTA-treated vs. acid-etched dentin using ethanol wet-bonding. Part II: Effects of mechanical cycling load on microtensile bond strengths. *Dent Mater* **27**, 563–572.

Schulze, K.A., Oliveira, S.A., Wilson, R.S., Gansky, S.A., Marshall, G.W. & Marshall, S.J. (2005). Effect of hydration variability on hybrid layer properties of a self-etching versus an acid-etching system. *Biomaterials* **26**, 1011–1018.

Takahashi, A., Sato, Y., Uno, S., Pereira, P.N. & Sano, H. (2002). Effects of mechanical properties of adhesive resins on bond strength to dentin. *Dent Mater* **18**, 263–268.

Takahashi, R., Nikaido, T., Ariyoshi, M., Foxton, R.M. & Tagami, J. (2010). Microtensile bond strengths of a dual-cure resin cement to dentin resin-coated with an all-in-one adhesive system using two curing modes. *Dent Mater* **29**, 268–277.

Tay, F.R., Gwinnett, J.A. & Wei, S.H. (1996). Micromorphological spectrum from overdrying to overwetting acid-conditioned dentin in water-free acetone-based, single-bottle primer/adhesives. *Dent Mater* **12**, 236–244.

Tay, F.R. & Pashley, D.H. (2001). Aggressiveness of contemporary self-etching systems. I: Depth of penetration beyond dentin smear layers. *Dent Mater* **17**, 296–308.

Tay, F.R. & Pashley, D.H. (2003). Have dentin adhesives become too hydrophilic? *J Can Dent Assoc* **69**, 726–731.

Toledano, M., Cabello, I., Yamauti, M. & Osorio, R. (2012a). Differential resin-dentin bonds created after caries removal with polymer burs. *Microsc Microanal* **18**, 1–12.

Toledano, M., Osorio, R., Albaladejo, A., Aguilera, F.S. & Osorio, E. (2006). Differential effect of *in vitro* degradation on resin-dentin bonds produced by self-etch versus total-etch adhesives. *J Biomed Mater Res A* **77**, 128–135.

Toledano, M., Osorio, R., Osorio, E., Aguilera, F.S., Yamauti, M., Pashley, D.H. & Tay, F. (2007). Durability of resin-dentin bonds: Effects of direct/indirect exposure and storage media. *Dent Mater* **23**, 885–892.

Toledano, M., Perdigão, J., Osorio, R. & Osorio, E. (2000). Effect of dentin deproteinization on microleakage of class V composite restorations. *Oper Dent* **25**, 497–504.

Toledano, M., Yamauti, M., Osorio, E., Monticelli, F. & Osorio, R. (2012b). Characterization of micro- and nanophase separation of dentin bonding agents by stereoscopy and atomic force microscopy. *Microsc Microanal* **3**, 1–10.

Uehara, K. & Sakurai, M. (2002). Bonding strength of adhesives and surface roughness of joined parts. *J Mater Process Technol* **127**, 178–181.

Uekusa, S., Yamaguchi, K., Miyazaki, M., Tsubota, K., Kurokawa, H. & Hosoya, Y. (2006). Bonding efficacy of single-step self-etch systems to sound primary and permanent tooth dentin. *Oper Dent* **31**, 569–576.

Van Landuyt, K.L., De Munck, J., Snauwaert, J., Coutinho, E., Poitevin, A., Yoshida, Y., Inoue, S., Peumans, M., Suzuki, K., Lambrechts, P. & Van Meerbeek, B. (2005). Monomer-solvent phase separation in one-step self-etch adhesives. *J Dent Res* **84**, 183–188.

Van Landuyt, K.L., Snauwaert, J., De Munck, J., Peumans, M., Yoshida, Y., Poitevin, A., Coutinho, E., Suzuki, K., Lambrechts, P. & Van Meerbeek, B. (2007). Systematic review of the chemical composition of contemporary dental adhesives. *Biomaterials* **28**, 3757–3785.

Van Meerbeek, B., De Munck, J., Yoshida, Y., Inoue, S., Vargas, M., Vijay, P., Van Landuyt, K., Lambrechts, P. & Vanherle, G. (2003). Buonocore memorial lecture. Adhesion to enamel and dentin: Current status and future challenges. *Oper Dent* **28**, 215–235.

Van Meerbeek, B., Van Landuyt, K., De Munck, J., Hashimoto, M., Peumans, M., Lambrechts, P., Yoshida, Y., Inoue, S. & Suzuki, K. (2005). Technique-sensitivity of contemporary adhesives. *Dent Mater* **24**, 1–13.

Van Strijp, A.J., Jansen, D.C., DeGroot, J., ten Cate, J.M. & Everts, V. (2003). Host-derived proteinases and degradation of dentine collagen *in situ*. *Caries Res* **37**, 58–65.

Yamauti, M., Hashimoto, M., Sano, H., Ohno, H., Carvalho, R.M., Kaga, M., Tagami, J., Oguchi, H. & Kubota, M. (2003). Degradation of resin-dentin bonds using NaOCl storage. *Dent Mater* **19**, 399–405.

Yiu, C.K., Pashley, E.L., Hiraishi, N., King, N.M., Goracci, C., Ferrari, M., Carvalho, R.M., Pashley, D.H. & Tay, F.R. (2005). Solvent and water retention in dental adhesive blends after evaporation. *Biomaterials* **26**, 6863–6872.

Yoshida, E., Hashimoto, M., Hori, M., Kaga, M., Sano, H. & Oguchi, H. (2004a). Deproteinizing effects on resin-tooth bond structures. *J Biomed Mater Res B Appl Biomater* **68**, 29–35.

Yoshida, Y., Nagakane, K., Fukuda, R., Nakayama, Y., Okazaki, M., Shintani, H., Inoue, S., Tagawa, Y., Suzuki, K., De Munck, J. & Van Meerbeek, B. (2004b). Comparative study on adhesive performance of functional monomers. *J Dent Res* **83**, 454–458.

Zhou, X.D., Zhang, S.C., Huebner, W. & Ownby, P.D. (2001). Effect of the solvent on the particle morphology of spray PMMA. *J Mater Sci* **36**, 3759–3768.